ChemComm

COMMUNICATION

View Article Online
View Journal | View Issue

Cite this: *Chem. Commun.*, 2021, **57**, 13305

Received 6th October 2021,
Accepted 9th November 2021

DOI: 10.1039/d1cc05640a

rsc.li/chemcomm

Experimental and theoretical evidence of attractive interactions between dianions: $[PdCl_4]^{2-}\cdots[PdCl_4]^{2-}$†

Wiktor Zierkiewicz, *[a] Mariusz Michalczyk, *[a] Thierry Maris, [b] Rafał Wysokiński [a] and Steve Scheiner [c]

Inspection of the arrangement of tetrachloridopalladate(II) centers in a crystalline solid places the Cl of one $[PdCl_4]^{2-}$ directly above the Pd center of its neighbor. A survey of the CSD provides 22 more examples of such $MX_4^{2-}\cdots MX_4^{2-}$ complexes, with M being a Group 10 metal and X = Cl, Br, or I. Quantum calculations attribute this arrangement to a π-hole bond wherein Cl lone pairs of one unit transfer charge to vacant orbitals above the Pd center of its neighbor. The stabilizing effect of this bond must overcome the strong Coulombic repulsion between the two dianions, which is facilitated by a polarizable environment as would be present in a crystal, but much more so when the effects of the neighboring counterions are factored in. These conclusions are extended to other $[MX_4]^{2-}$ homodimers, where M represents other members of Group 10, namely Ni and Pt.

Amongst the crystal structures presented over the last few years that contained Pd,[1–11] one of the more interesting is a self-assembling structural motif wherein halogens are attached to Pd as a building block for perovskite materials used in optoelectronics due to their strong absorption in the visible spectral range, good band gap and promising photoelectric response.[9,10] Other Pd clusters have potential antitumor, antimetastatic and radioprotective activities.[2,3] There are previous literature reports demonstrating the ability of square planar palladium complexes to serve as σ-hole/π-hole acceptors.[12–16] However, as the monomeric $PdCl_4^{2-}$ unit is planar, there arises the intriguing possibility of the existence of a π-hole above the Pd atom, which represents an electrostatic potential which is positive or considerably less negative than that surrounding the remainder of the anion.[17–22] It is just this sort of π-hole that is the origin of triel and other noncovalent bonds to planar units,[23] so there is reason to wonder if such an attractive interaction might occur for $PdCl_4^{2-}$ and perhaps other related anions.

Although π-hole bonds between anions have not been observed previously for the Pd family, we were encouraged in this idea by earlier observations in ionic liquids[24] or between anions in aspartate dimers.[25] More closely related are anion–anion complexes[26–33] that involve the Zn family, alkaline earth metals, and triel, pnicogen, and aerogen atoms.[34–40] Nevertheless, the double negative charge of PdX_4^{2-} presents a real challenge to any such interactions. The results reported below provide the first evidence that pairs of dianions can overcome their powerful mutual coulombic repulsion so as to engage in attractive interactions with each other.

This study begins with the atomic arrangement within a crystal that was first synthesized and then studied using diffraction methods. Of most interest are the relative dispositions of various tetrachloridopalladate(II) centers, as depicted in Fig. 1.

A Cl atom of one unit lies directly above the Pd of its neighbor, with a R(Pd···Cl) distance of 3.181 Å, quite a bit smaller than the sum of their vdW radii of 3.97 Å.[41] The normalized contact (Nc)[42] ratio between the actual distance and this vdW sum is 0.80, significantly shorter than the Au···Cl and Au···O coinage bond contacts of 0.88 and 0.95, respectively, in an analogous tetrachloridoaurate(III) crystal.[42]

The molecular electrostatic potential (MEP) surrounding each monomer is displayed in Fig. 2. The MEP of $[PdCl_4]^{2-}$ is negative on the extensions of the four Pd–Cl bonds, as well as above the Pd center which can be considered a π-hole, despite its negative value of −0.30 au. There are also less negative regions as belts surrounding the Cl atoms, but these areas do not correspond to the maxima of the MEP.

[a] *Faculty of Chemistry Wrocław University of Science and Technology Wybrzeże Wyspiańskiego 27, 50-370 Wrocław, Poland.*
E-mail: wiktor.zierkiewicz@pwr.edu.pl, mariusz.michalczyk@pwr.edu.pl
[b] *Département de Chimie, Université de Montréal, Montréal, Québec, H3C 3J7, Canada*
[c] *Department of Chemistry and Biochemistry Utah State University, Logan, Utah 84322-0300, USA*

† Electronic supplementary information (ESI) available. CCDC 2109436. For ESI and crystallographic data in CIF or other electronic format see DOI: 10.1039/d1cc05640a

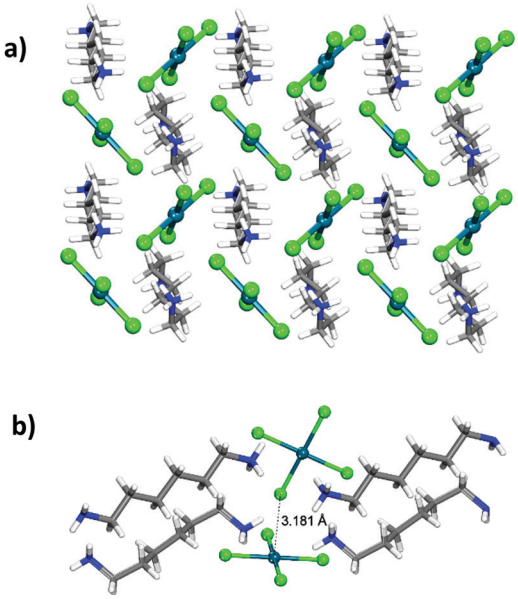

Fig. 1 The geometry of the source crystal structure: (a) representation of the extended structural motif in the crystal solid and (b) a $[NH_3–(CH_2)_6–NH_2]_4[PdCl_4]_2$ unit; the anionic subunits are presented as ball and sticks, while counterions as capped sticks; hydrogen bonds are omitted for clarity. Coloring of atoms: Pd – dark green, Cl – light green, N – blue, C – grey, H – white.

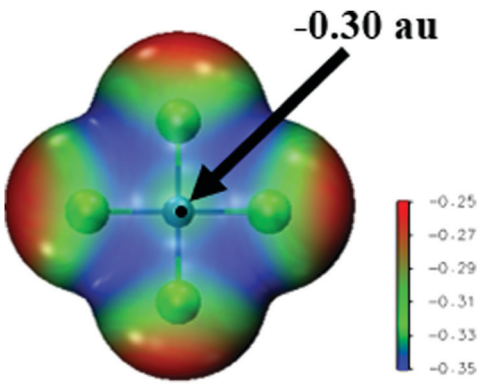

Fig. 2 MEP of the $[PdCl_4]^{2-}$ monomer on the 0.001 au isodensity surface. The black dot indicates $V_{s,max}$ on the Pd atom (π-hole); values on the color bar are given in au.

As a first approximation toward understanding the sorts of bonding within the crystal, the interaction energy between a pair of naked $PdCl_4^{2-}$ units with their coordinates taken from the crystal was evaluated to be +211.8 kcal mol^{-1}. Such a high positive quantity is reflective of the Coulombic repulsion between two units of like charge −2. It is of note, however, that the repulsion is much higher, +417.7 kcal mol^{-1}, if the interaction is grossly simplified to a pair of point charges placed at the positions of the Pd and Cl atoms, so there is an initial indication of some sort of stabilizing force.

It is clear that the diamine counterions would help to disperse the negative charge of the $PdCl_4^{2-}$ units. This effect was modeled by placing a pair of $[NH_3(CH_2)_6NH_2]^+$ counterions on each dianion, again using crystal coordinates, leading to the structure illustrated in Fig. 1b. These cations have a large effect on the MEP, raising the potential of the Pd π-hole of each triad by 140 kcal mol^{-1}, up to −54.8 kcal mol^{-1}. This rise is not an artifact of the choice of a particular isodensity surface on which to measure V_{max}. As can be seen in Fig. S1 (ESI†), this large difference is characteristic of the entire range of distance above the central Pd nucleus. There is also a change in the MEP surrounding the Cl atoms, with V_{min} going from −202 kcal mol^{-1} in the naked $PdCl_4^{2-}$ to −70 kcal mol^{-1} in the triad. Most importantly, the addition of the counterions turned a repulsive potential into an attractive one, with a negative interaction energy of −100.4 kcal mol^{-1}. In other words, these counterions provide an enormous stabilizing component, swinging the interaction energy by more than 300 kcal mol^{-1}. In fact, a partial optimization of the geometry of this hexamer, focusing on the intermolecular distance, causes the two triads to approach even more closely than in the X-ray structure, with R(Pd···Cl) shrinking down to 2.955 Å.

Regarding this stabilizing effect, it is largely electrostatic. To be more specific, decomposition of the total interaction energy was carried out for the bare dianion pair and for that combining a pair of triads, each with two positive counterions. The electrostatic component was a repulsive +220 kcal mol^{-1} for the former, but became attractive at −66 kcal mol^{-1} for the latter. There were also enhancements of the orbital interaction (13 kcal mol^{-1}) and dispersion (19 kcal mol^{-1}) energies, but these changes pale in comparison with the electrostatic stabilization. A similar effect of decreasing Coulombic repulsion between the cationic centers of indium(III) species was reported elsewhere.[43]

In order to amplify these strong electrostatic effects, each of the counterions was replaced by a constellation of point charges. Each such charge was superimposed upon the atom position and was assigned a charge equal to the natural charge of that atom within the full counterion. Again, each monomer was paired with two constellations of point charges, approximating the full counterion. The interaction energy of these two subsystems with each other was computed to be −100.5 kcal mol^{-1}. In other words, the counterions are effective at converting a repulsive interaction between two bare $PdCl_4^{2-}$ dianions into an attractive one, even if they are treated only as point charges. Note that the approximation by point charges avoids the possibility of stabilization by dispersion or any possible H···H interactions. Even if the counterions are further simplified, each to only a single point charge, at the position of the most proximate N atom, with a charge of +1, the results are very similar, with the interaction energy equal to −100.4 kcal mol^{-1}.

While one might attribute the reversal of the repulsion to the attenuation of the charge on the $PdCl_4^{2-}$ dianions, the very attractive negative interaction energy is strongly suggestive of specific noncovalent bonding. The first step in identifying any such bonds is taken by analysis of the electron density topology. The QTAIM analysis of the density of the full hexamer is displayed in Fig. 3 where bond paths are indicated by broken lines.

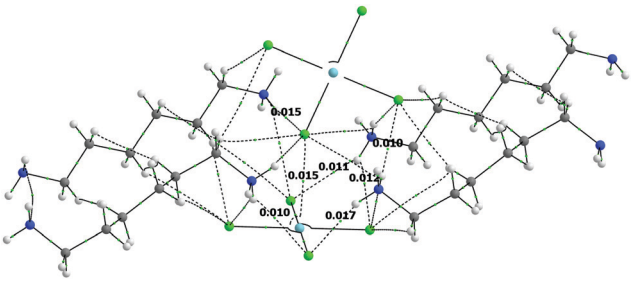

Fig. 3 QTAIM bond critical points (green dots) and bond paths (dashed lines) for the limited fragment of the $[NH_3–(CH_2)_6–NH_2]_4[PdCl_4]_2$ system. Selected ρ at BCPs with values ≥0.010 are reported in au.

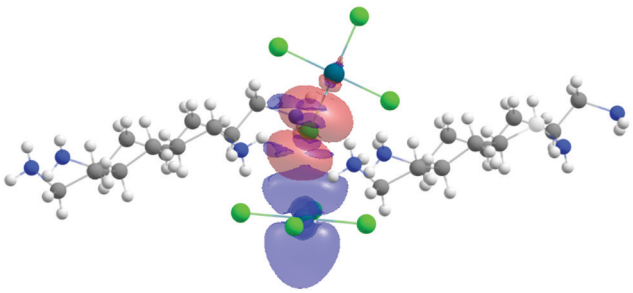

Fig. 5 The isosurface (on the 0.001 isovalue) of two of the interacting orbitals [LP(Cl) → RY(Pd)] with the largest E^2 (1.79 kcal mol^{-1}). The LP(Cl) orbital is orange-colored, while RY(Pd) is blue.

The value of the density at each bond critical point that is larger than 0.01 is reported as well. (A full molecular diagram showing all bond path densities is presented in Fig. S2, ESI.†) First and foremost, there is a clear bond between the Pd of one unit and a Cl from its partner, with ρ = 0.015, typical of noncovalent interactions.[44–46] This is not the only bond, as there appear to also be a number of NH···Cl H-bonds, and several that link the central Pd with an NH group on a counterion, but most have a smaller ρ_{BCP}. A comparison can be drawn with the tetrachloridoaurate(III)-based complex,[42] which had smaller densities in the range of 0.006–0.011 au. Complementary to QTAIM is the NCI protocol which depicts noncovalent interactions *via* a color scheme. The green disks in Fig. 4 are clear evidence of a principal Pd···Cl interaction, with smaller blots that correspond to the aforementioned interactions involving H atoms.

Another window into the nature of the bonding arises in connection with NBO[47] which focuses on small charge transfers between individual orbitals. Of those involving the two $PdCl_4^{2-}$ units, Fig. 5 depicts the overlap between a lone pair on the Cl atom (shown in red) and a vacant Rydberg orbital on Pd of the other (blue), best characterized as an empty p-orbital. This particular Cl → Pd transfer, along with similar such pairs, contributes 6.2 kcal mol^{-1}, while another 4.5 kcal mol^{-1} is added by transfers to the vacant σ*(PdCl) orbitals. These sorts of interorbital transfers from Lewis bases to acids are signposts of noncovalent bonds.

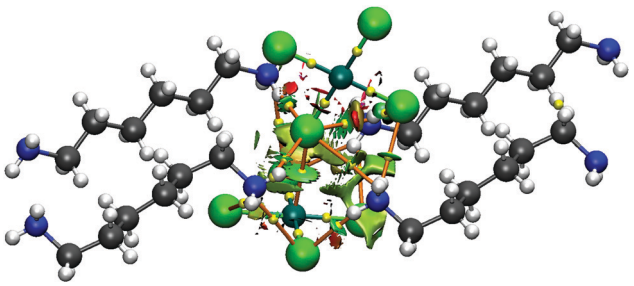

Fig. 4 QTAIM bond critical points (yellow dots) and bond paths (orange sticks) along with the NCI isosurfaces (green spheres represent noncovalent interaction regions) at the RDG 0.5 au isovalue for the limited fragment of the $[NH_3–(CH_2)_6–NH_2]_4[PdCl_4]_2$ system containing the discussed interactions.

In order to place these findings in a broader context, the calculations considered Ni and Pt, which are other members of the Group 10 family. Like $PdCl_4^{2-}$, the two related MCl_4^{2-} dianions are also surrounded by a fully negative MEP so any π-hole will also be negative, and the values are in fact −191.3 and −196.6 kcal mol^{-1} for Ni and Pt, respectively. Although homodimers of each of these dianions are unstable in the gas phase, true minima were obtained when they were placed in a polarizable dielectric continuum with ε = 78 to simulate water. These structures are displayed in Fig. S3 (ESI†) and have R(M···Cl) distances of 3.835, 3.808, and 4.075 Å for Ni, Pd, and Pt, respectively, all shorter than the sum of their vdW radii. The Pd···Cl distance of 3.808 Å is considerably longer than that within the crystal (3.181 Å). This lengthening highlights the fact that aqueous solvation can only partly account for the full effects of a crystal environment. The longer intermolecular distances are also reflected in small ρ_{BCP} values as can be seen in Fig. S2 and Table S2 (ESI†). According to Table S1 (ESI†), the interaction energies of these three homodimers are all slightly positive (∼2 kcal mol^{-1}), so are metastable with respect to dissociation to a pair of separate dianions, in the sense that a separation must overcome an energy barrier which was estimated to be less than 1.3 kcal mol^{-1}.

It is natural to wonder about the overall prevalence of interactions like these. A survey of the Cambridge Structural Database (CSD)[48] found 22 hits when searching crystal structures similar to those presented above. The search criteria were limited to $MX_4^{2-}\cdots MX_4^{2-}$ dimers (M = Ni, Pd, Pt; X = Cl, Br, I) with the nonbonded contact between M and X according to the internal software rules. Within the associated set of deposited crystals, the $[PdCl_4]^{2-}$ motif is the dominant one as it covers 77% of the total structures found. As a significant distinction, as many as 20 of the 22 structures contained Pd, two with Pt, and none with Ni. It must be stressed that in all crystals the monomer anionic unit maintained a square planar geometry, with an orthogonal disposition from one to the next. Fig. S5 (ESI†) displays several selected examples of these arrangements.

In conclusion, to the best of our knowledge the work described here presents the first clear experimental and theoretical evidence of an attractive interaction between two dianions, in this case involving tetrachloridopalladate(II) centers.

The major component of this attraction is a π-hole bond involving charge transfer from halogen lone pairs to a Group 10 metal atom within the context of a pair of $[MX_4]^{2-}$ dianions. This attraction is not possible in the gas phase, but does exist within the context of a polarizable medium such as an aqueous solvent. A more important factor, and one which permits a much stronger interaction, is the inclusion of the positive counterions that interact directly with these dianions in the crystal. Besides this particular $[PdCl_4]^{2-}$ system, there are a number of closely related Group 10 $[MX_4]^{2-}$ pairings identified within the CSD, most of which involve Pd. It is hoped that the ideas expressed here may open a new route to the future design of new supramolecular synthons containing Group 10 elements with properties useful for optoelectronic and photovoltaic applications, among others.

This work was financed in part by a statutory activity subsidy from the Polish Ministry of Science and Higher Education for the Faculty of Chemistry of Wroclaw University of Science and Technology and by the US National Science Foundation under Grant No. 1954310. A generous allotment of computer time from the Wroclaw Supercomputer and Networking Center is acknowledged.

Conflicts of interest

There are no conflicts to declare.

Notes and references

1 R. W. Berg and I. Sotofte, *Acta Chem. Scand., Ser. A*, 1976, **30**, 843–844.
2 I. A. Efimenko, A. V. Churakov, N. A. Ivanova, O. S. Erofeeva and L. I. Demina, *Russ. J. Inorg. Chem.*, 2017, **62**, 1469–1478.
3 I. A. Efimenko, M. V. Filimonova, A. V. Churakov, N. A. Ivanova, O. S. Erofeeva, A. S. Samsonova, T. S. Podosinnikova and A. S. Filimonov, *Russ. J. Coord. Chem.*, 2020, **46**, 339–349.
4 T. Maris, *Acta Crystallogr., Sect. E: Struct. Rep. Online*, 2008, **64**, m208.
5 T. Maris, G. Bravic, N. B. Chanh, J. M. Leger, J. C. Bissey, A. Villesuzanne, R. Zouari and A. Daoud, *J. Phys. Chem. Solids*, 1996, **57**, 1963–1975.
6 M. M. Olmstead, A. S. Ginwalla, B. C. Noll, D. S. Tinti and A. L. Balch, *J. Am. Chem. Soc.*, 1996, **118**, 7737–7745.
7 M. M. Olmstead, P. P. Wei and A. L. Balch, *Chem. – Eur. J.*, 1999, **5**, 3136–3142.
8 M. M. Olmstead, P. P. Wei, A. S. Ginwalla and A. L. Balch, *Inorg. Chem.*, 2000, **39**, 4555–4559.
9 M. K. Wong, F. Z. Liu, C. S. Kam, T. L. Leung, H. W. Tam, A. B. Djurisic, J. Popovic, H. K. Li, K. Shih, K. H. Low, W. K. Chan, W. Chen, Z. B. He, A. Ng and C. Surya, *Chem. Mater.*, 2017, **29**, 9946–9953.
10 H. W. Zhou, X. L. Cui, C. Yuan, J. W. Cui, S. Z. Shi, G. H. He, Y. Y. Wang, J. Z. Wei, X. P. Pu, W. Z. Li, D. F. Zhang, J. Wang, X. Z. Ren, H. Y. Ma, X. Shao, X. T. Wei, J. S. Zhao, X. X. Zhang and J. Yin, *ACS Omega*, 2018, **3**, 13960–13966.
11 R. Zouari, J. M. Leger, T. Maris and N. B. Chanh, *Acta Crystallogr., Sect. C: Cryst. Struct. Commun.*, 1998, **54**, 1253–1255.
12 S. V. Baykov, S. I. Filimonov, A. V. Rozhkov, A. S. Novikov, I. V. Ananyev, D. M. Ivanov and V. Y. Kukushkin, *Cryst. Growth Des.*, 2020, **20**, 995–1008.
13 D. M. Ivanov, N. A. Bokach, V. Y. Kukushkin and A. Frontera, *Chem. – Eur. J.*, 2021, **27**, DOI: 10.1002/chem.202103173.
14 E. A. Katlenok, M. Haukka, O. V. Levin, A. Frontera and V. Y. Kukushkin, *Chem. – Eur. J.*, 2020, **26**, 7692–7701.
15 A. V. Rozhkov, I. V. Ananyev, R. M. Gomila, A. Frontera and V. Y. Kukushkin, *Inorg. Chem.*, 2020, **59**, 9308–9314.
16 L. E. Zelenkov, A. A. Eliseeva, S. V. Baykov, V. V. Suslonov, B. Galmes, A. Frontera, V. Y. Kukushkin, D. M. Ivanov and N. A. Bokach, *Inorg. Chem. Front.*, 2021, **8**, 2505–2517.
17 P. Politzer and J. S. Murray, *J. Comput. Chem.*, 2018, **39**, 464–471.
18 J. S. Murray, P. Lane, T. Clark, K. E. Riley and P. Politzer, *J. Mol. Model.*, 2012, **18**, 541–548.
19 H. Wang, W. Wang and W. J. Jin, *Chem. Rev.*, 2016, **116**, 5072–5104.
20 A. Bauza, T. J. Mooibroek and A. Frontera, *Chem. Phys. Chem.*, 2015, **16**, 2496–2517.
21 T. J. Mooibroek, *Chem. Phys. Chem.*, 2021, **22**, 141–153.
22 A. Bauza, T. J. Mooibroek and A. Frontera, *CrystEngComm*, 2016, **18**, 10–23.
23 S. J. Grabowski, *Molecules*, 2015, **20**, 11297–11316.
24 S. H. Ganatra, V. R. Shaikh, A. S. Ujjankar, S. D. Khobragade, P. A. Tomar and K. J. Patil, *J. Mol. Liq.*, 2020, **315**, 113654.
25 M. O. Miranda, D. J. R. Duarte and I. Alkorta, *Chem. Phys. Chem.*, 2020, **21**, 1052–1059.
26 D. Quinonero, I. Alkorta and J. Elguero, *Phys. Chem. Chem. Phys.*, 2016, **18**, 27939–27950.
27 R. Prohens, A. Portell, M. Font-Bardia, A. Bauza and A. Frontera, *Chem. Commun.*, 2018, **54**, 1841–1844.
28 I. Alkorta, I. Mata, E. Molins and E. Espinosa, *Chem. – Eur. J.*, 2016, **22**, 9226–9234.
29 L. M. Azofra, J. Elguero and I. Alkorta, *Phys. Chem. Chem. Phys.*, 2020, **22**, 11348–11353.
30 L. M. Azofra, J. Elguero and I. Alkorta, *J. Phys. Chem. A*, 2020, **124**, 2207–2214.
31 I. Mata, E. Molins, I. Alkorta and E. Espinosa, *J. Phys. Chem. A*, 2015, **119**, 183–194.
32 O. Mo, M. M. Montero-Campillo, M. Yanez, I. Alkorta and J. Elguero, *J. Phys. Chem. A*, 2020, **124**, 1515–1521.
33 E. Navarro-Garcia, B. Galmes, M. D. Velasco, A. Frontera and A. Caballero, *Chem. – Eur. J.*, 2020, **26**, 4706–4713.
34 R. Wysokinski, W. Zierkiewicz, M. Michalczyk and S. Scheiner, *Chem. Phys. Chem.*, 2020, **21**, 1119–1125.
35 R. Wysokinski, W. Zierkiewicz, M. Michalczyk and S. Scheiner, *J. Phys. Chem. A*, 2020, **124**, 2046–2056.
36 W. Zierkiewicz, R. Wysokinski, M. Michalczyk and S. Scheiner, *Chem. Phys. Chem.*, 2020, **21**, 870–877.
37 R. Wysokiński, W. Zierkiewicz, M. Michalczyk and S. Scheiner, *Phys. Chem. Chem. Phys.*, 2021, **23**, 13853–13861.
38 R. Wysokinski, W. Zierkiewicz, M. Michalczyk and S. Scheiner, *Chem. Phys. Chem.*, 2021, **22**, 818–821.
39 R. Wysokinski, M. Michalczyk, W. Zierkiewicz and S. Scheiner, *Phys. Chem. Chem. Phys.*, 2021, **23**, 4818–4828.
40 A. Grabarz, M. Michalczyk, W. Zierkiewicz and S. Scheiner, *Molecules*, 2021, **26**, 2116.
41 S. Alvarez, *Dalton Trans.*, 2013, **42**, 8617–8636.
42 A. Daolio, A. Pizzi, G. Terraneo, M. Ursini, A. Frontera and G. Resnati, *Angew. Chem., Int. Ed.*, 2021, **60**, 14385–14389.
43 J. Echeverría, *Chem. Commun.*, 2018, **54**, 6312–6315.
44 R. Bader, Atoms In Molecules. *A Quantum Theory*, Clarendon Press, Oxford, 1990.
45 R. F. W. Bader, *J. Phys. Chem. A*, 1998, **102**, 7314–7323.
46 F. Cortés-Guzmán and R. F. W. Bader, *Complementarity of QTAIM and MO theory in the study of bonding in donor–acceptor complexes*, 2005.
47 F. Weinhold, C. R. Landis and E. D. Glendening, *Int. Rev. Phys. Chem.*, 2016, **35**, 399–440.
48 C. R. Groom, I. J. Bruno, M. P. Lightfoot and S. C. Ward, *Acta Crystallogr., Sect. B: Struct. Sci., Cryst. Eng. Mater.*, 2016, **72**, 171–179.

